PCCP

COMMUNICATION

A Theoretical Investigation of Internal Conversion in 1,2-Dithiane Using Non-Adiabatic Multiconfigurational Molecular Dynamics

Received 00th January 20xx,
Accepted 00th January 20xx

DOI: 10.1039/x0xx00000x

www.rsc.org/

C. D. Rankine,[a] J. P. F. Nunes,[a] M. S. Robinson,[a,b] P. D. Lane[a,c] and D. A. Wann*[a]

Non-adiabatic multiconfigurational molecular dynamics simulations have revealed a molecular "Newton's Cradle" that activates on absorption of light in the mid-UV and assists the S_1/S_0 internal conversion process in 1,2-dithiane, protecting the disulfide bond from photodamage. This communication challenges contemporary understanding of the S_1/S_0 internal conversion process in 1,2-dithiane and presents a classically-intuitive reinterpretation of experimental evidence.

The disulfide bond is ubiquitous in the natural world and, for some specialised proteins, certain disulfide bonds are key to their survival under extreme conditions.[1]

Hot springs and deep-sea hydrothermal vents are considered among the most extreme environments on Earth, and many Archaea that thrive under these conditions share a common set of protein adaptations. An increased number of disulfide bonds is known to be among this set, allowing for the retention of functionality at elevated temperatures.[2-5]

In proteins that are likely to be exposed to harsh solar radiation, disulfide bonds are often found neighbouring tryptophan residues.[6] Here, disulfide bonds can confer photostability by acting as a sink to quench harmful UV-induced fluorescence originating from the tryptophan residues.[7-9]

Despite this, disulfide bonds in small aliphatic acyclic disulfides are neither innately stable to heat[10] nor to light[11-13] in the mid-UV. Although disulfide bonds are typically stronger than the neighbouring sulfur-carbon bonds,[13] studies have demonstrated that fission of the disulfide bond is facile using light in the mid-UV[11-13] and takes place *via* a sub-picosecond electronically-excited photochemical pathway on the S_1 surface,[14] generating $^{\bullet}$SR radicals with an appreciable quantum yield. In contrast, small aliphatic cyclic disulfides appear comparatively photostable, leading some to speculate that the photostability of the disulfide bond is a topological property (Scheme 1).[9,15,16]

The contemporary understanding of one such species – one of the simplest cyclic disulfides, 1,2-dithiane – is that fission of the disulfide bond generates the $^{\bullet}$S-$(CH_2)_4$-S$^{\bullet}$ diradical, but the species exists only transiently. The S_1 and S_0 states couple *via* a minimal-energy conical intersection (MECI) along the sulfur-sulfur stretching coordinate; this coordinate is activated upon electronic excitation and funnels S_1-1,2-dithiane towards the S_1/S_0 MECI, allowing the system to make a non-radiative return to the S_0 state. The electronic excitation energy is converted into S_0-state vibrational energy that can be harmlessly thermalised to the environment.[9,15,16] Since the internal conversion process outcompetes intramolecular vibrational relaxation (IVR) and returning to the S_0 state recouples the $^{\bullet}$S termini, the disulfide bond is scavenged before the structural integrity of the system is irreversibly lost.

The elegant ultrafast mass spectrometric (UMS) study[15] of Stephansen *et al.* captures the internal conversion process in action. An oscillating ion current signal was recorded post-photoexcitation – as clear an indicator of ultrafast photo-induced motion as is possible in a UMS experiment. The motion was assigned to a low-frequency normal mode translating the system along the sulfur-sulfur coordinate between a shallow S_1 minimum and the nearby S_1/S_0 MECI.

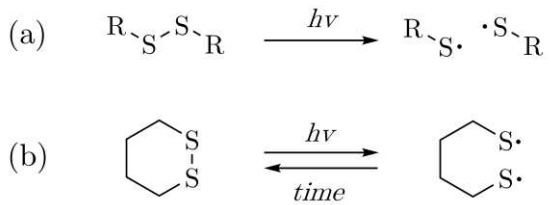

Scheme 1: The photolytic fission of the disulfide bond in a) an aliphatic acyclic disulfide and b) the aliphatic cyclic disulfide 1,2-dithiane.

[a] Department of Chemistry, University of York, Heslington, York, YO10 5DD, UK
[b] Current Address: Department of Physics and Astronomy, The University of Nebraska-Lincoln, Lincoln, Nebraska, NE 68588, USA
[c] Current Address: School of Engineering and Physical Sciences, Heriot-Watt University, Edinburgh, EH14 4AS, UK
* Address correspondence to derek.wann@york.ac.uk

Electronic Supplementary Information (ESI) available: additional computational details, orbitals included in our SA3-CASSCF(10,8) active space (Fig. S1), *.xyz* geometries (Tables S1-3), LIIC pathways computed at the SA3-CASSCF(10,8) and LS-XMS-CASPT2 levels and supplementary two-dimensional heat-density maps (Fig. S2) characterising the motion reported in this communication.

Accompanying *ab initio* calculations confirmed that both waypoints were situated in a flat, featureless S_1/S_0 coupling region (CR) on the S_1 surface.

In this communication, we report a classically-intuitive reinterpretation of the internal conversion process in 1,2-dithiane as revealed by our non-adiabatic multiconfigurational molecular dynamics (NAMMD)[17] simulations. Readers unfamiliar with this approach are directed to Refs. 18 and 19. A molecular "Newton's Cradle" (Fig. 1) is revealed that is activated on absorption of light in the mid-UV and allows 1,2-dithiane to periodically pass over an extended S_1/S_0 CR (Fig. 2). It is easy to understand this motion in the context of a two-dimensional phase space defined in terms of the principal degrees of freedom involved, namely the *r*S-S and *d*C-C-C-C internal coordinates. *r*S-S is mapped from 2 to 8 Å and *d*C-C-C-C is mapped from 0 to 360°, the latter allowing for the separation in phase space of systems in which *d*C-C-C-C rotates past 180° and continues towards (and beyond) 360° and in which *d*C-C-C-C approaches 180° and turns back towards 0°.

Our NAMMD simulations were recorded at the SA3-CASSCF(10,8)/def2-SV(P)[20] (Fig. S1) level using the NEWTON-X[21] package interfaced with COLUMBUS v7.0.[22] The suitability of the SA3-CASSCF(10,8)/def2-SV(P) approach has been verified by further calculations at the LS-XMS-CASPT2 level (Fig. S2). Details are given in the supplementary information. All analytical gradients[23] and non-adiabatic coupling vectors[24] are computed in accordance with the integrated routines, and non-adiabatic transition probabilities were accounted for using an augmented fewest-switches algorithm.[25] Each member of a Wigner-distributed ensemble[26] containing fifty unique S_0-state starting structures was individually transformed into the S_1 state according to a computed transition energy and transition moment. Each system was subsequently propagated through time for 750 fs using a 0.5 fs integration time step *via* the velocity-Verlet algorithm.[27]

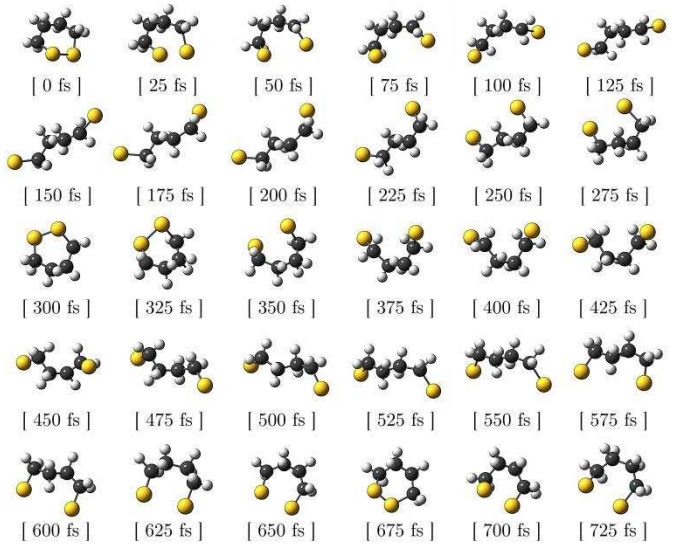

Figure 1: A series of stop-motion frames from a single NAMMD simulation representative of the molecular "Newton's Cradle".

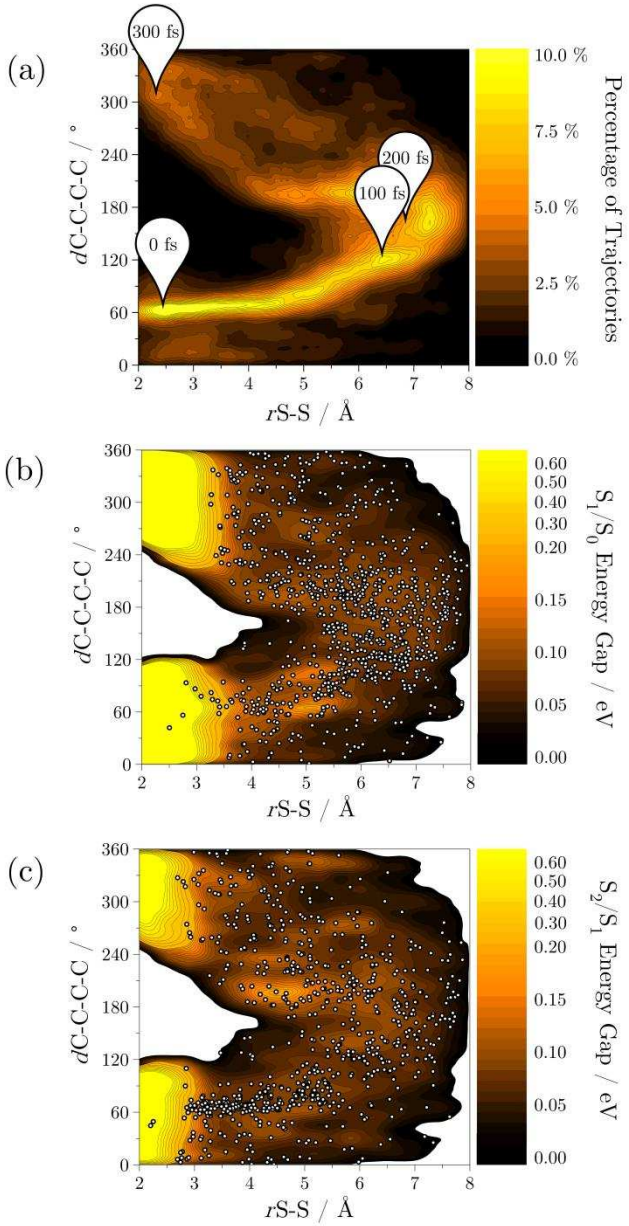

Figure 2: (a) A heat-density map of the percentage of NAMMD trajectories visiting a given segment of phase space. Data are derived from 50 independent NAMMD simulations recorded for 750 fs. The locations of the 0, 100, 200 and 300 fs structures from Fig. 1 are tagged. (b) A two-dimensional map of the energy gap between the S_1 and S_0 states. Sites where bidirectional S_1/S_0 surface-hopping events occur are indicated by circles. White regions of phase space are not visited by any NAMMD trajectories and no data are available for these regions. (c) As in (b), but for the S_2 and S_1 states.

No evidence is found in any of our NAMMD simulations for the spatial localisation of the system to the phase space surrounding the S_1 minimum or the neighbouring S_1/S_0 MECI. Our accompanying *ab initio* calculations (summarised in Tables S1-3) compute the two waypoints to lie >2.2 eV lower in energy than the Franck-Condon point on the S_1 surface (Fig. 3); the $^{\bullet}$S termini accumulate sufficient momentum in opposing directions on descent into the S_1/S_0 CR to pass by both waypoints.

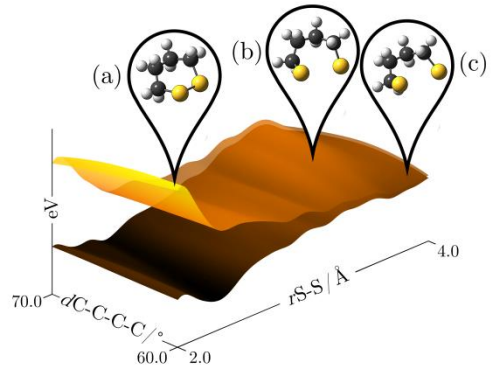

Figure 3: A slice of the S_0 and S_1 surfaces, approximated from our NAMMD simulations. The a) Franck-Condon point, b) neighbouring S_1 minimum, and c) S_1/S_0 MECI are indicated.

Our NAMMD simulations indicate that the S_1/S_0 MECI is unimportant to the S_1/S_0 internal conversion process. The S_1/S_0 CR is so extensive and associated with such a high degree of multireference character and interstate coupling that bidirectional S_2/S_1 and S_1/S_0 surface-hopping events are frequent throughout the region (Fig. 2b/2c).

An analysis of the average adiabatic population of the three lowest-energy singlet states expressed as a function of time (Fig. 4) shows that these surface-hopping events lead to equilibration of the states on the ultrafast timescale.

The threshold of the S_1/S_0 CR (defined arbitrarily as the point at which the separation in energy of the S_1 and S_0 states along the sulfur-sulfur stretching coordinate is less than the average separation at which S_1/S_0 surface-hopping events are observed) may be reached as early as 65.0 ± 15.5 fs post-photoexcitation. Travelling over the threshold into the S_1/S_0 CR is accompanied by an appreciable transfer of population into the S_0 state. Efficient equilibration of the three lowest-energy singlet states follows, even when the system is energetically (Fig. 5) and topologically isolated from the S_1/S_0 MECI.

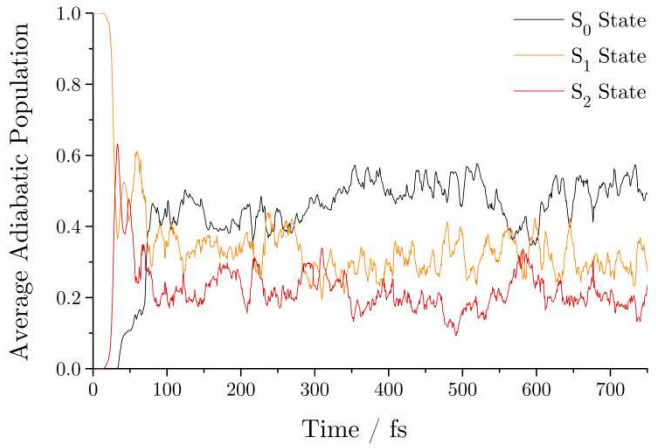

Figure 4: The average adiabatic populations of the three lowest-energy singlet states expressed as a function of time.

In <100 fs, the S_0 state is established as the dominantly-occupied state; this is critical to successful recoupling of the $^{\bullet}$S termini. For successful recoupling, the system needs not only to return to the S_0 state but for the $^{\bullet}$S termini to return into proximity. The S_1/S_0 CR comprises only the phase space associated with values of *r*S-S greater than 5.10 ± 0.70 Å. At smaller values of *r*S-S, approaching the S_0 equilibrium bonded value, surface-hopping events are prohibited by both the energy gap and low interstate coupling between the S_1 and S_0 states. The consequence is that surface-hopping events returning the system to the S_0 state are not possible in the immediate moments before collision of the $^{\bullet}$S termini; an ensemble of systems in the S_0 state needs to be prepared in advance of each collision event. Travelling through the S_1/S_0 CR ensures that, at any time, approximately 50% of the NAMMD ensemble is in the S_0 state and is able to attempt recoupling upon collision.

Our interpretation accounts for the origin of the components used to fit the UMS ion current signal recorded by Stephansen *et al.*[15]

The positions of peaks and troughs in the evolution of the *r*S-S internal coordinate expressed as a function of time (Fig. 6) match those in the inverse of the UMS ion current signal recorded Stephansen *et al.*[15] From the fitting of a damped sine function to an average wavepacket representative of our motion, a period of 349.6 fs is determined. This is in acceptable agreement with the period of 411 ± 27 fs reported by Stephansen *et al.*, considering the approximations made in order to fit the UMS data and, additionally, that the timescale of our NAMMD simulations is less than half the timescale of the UMS experiment. The period of our motion is seen to lengthen slightly with each cycle as a consequence of IVR; a longer timescale predictably results in the determination of a longer average period.

This process, ultimately leading to the ergodic exploration of phase space on a sufficiently long timescale, results in the stark loss of coherence in the ensemble of wavepackets (Fig. 6) on the NAMMD timescale. The average wavepacket is consequently damped, in line with experimental observations.

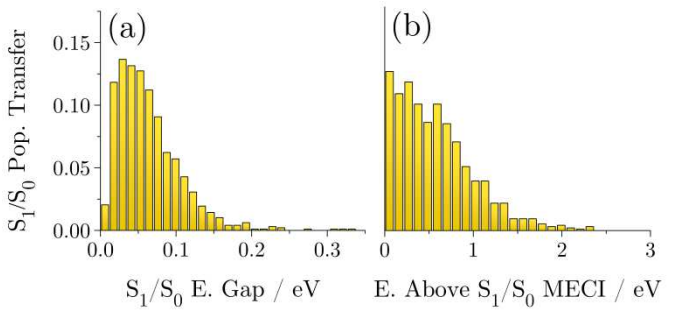

Figure 5: Histograms showing a) the bi-directional population transfer between the S_1 and S_0 states expressed as a function of the energy gap between those states, and b) the unidirectional population transfer from the S_1 state into the S_0 state as a function of the energy of the S_1 state above the S_1/S_0 MECI.

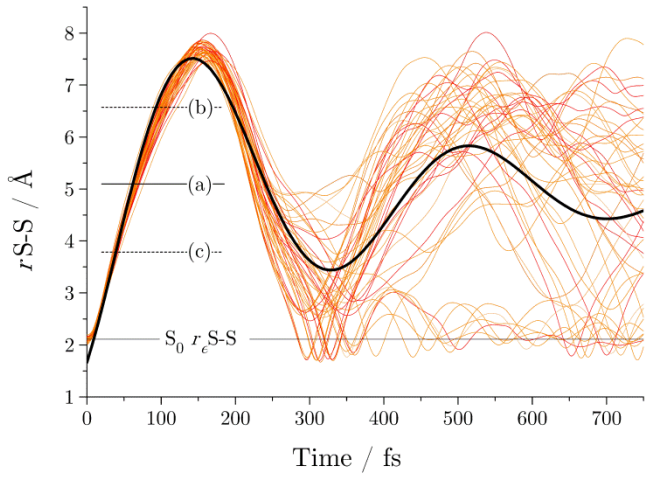

Figure 6: The evolution of the *r*S-S internal coordinate expressed as a function of time. Individual NAMMD trajectories are plotted in orange; a damped sine function fitted to the average NAMMD trajectory is plotted in black. The S_0-state equilibrium value for the *r*S-S internal coordinate (S_0 r_eS-S) computed at the SA3-CASSCF(10,8) level is indicated, as is a) the average value of the *r*S-S internal coordinate associated with the S_1/S_0 CR threshold (defined in text), b) the upper limit and c) the lower limit for the position of the S_1/S_0 CR threshold.

Note how, for a fraction of NAMMD simulations, successful recoupling of the $^{\bullet}$S termini occurs on the first collision. 5/50 systems return vibrationally hot to the S_0 state with an intact disulfide bond on the NAMMD timescale and do not re-enter the S_1/S_0 CR; they can be recognised in Fig. 6 by their characteristic wavepackets that, after the first collision event, oscillate around the calculated S_0 equilibrium S-S separation, r_eS-S, of 2.11 Å.

Irreversibly leaving the S_1/S_0 CR is non-trivial, evidenced by the low recovery rate of intact disulfides. An analysis of our NAMMD data has revealed three explanations.

The evolution of the *d*C-C-C-C internal coordinate expressed as a function of time is phase-shifted with respect to the evolution of the *r*S-S internal coordinate. The former internal coordinate first peaks in value at 207.8 ± 15.0 fs and the latter first peaks in value at 155.9 ± 6.6 fs. The consequence is that a slightly larger region of phase space is typically sampled during the ring-closing half-period of our motion than during the ring-opening half-period (Fig. S3). This can turn collision events into near misses from which it is difficult for the system to recover. As time elapses and other degrees of freedom are activated by IVR, it becomes increasingly unlikely for the $^{\bullet}$S termini to return into proximity. 7/50 systems miss their first collision and are not seen to leave the S_1/S_0 CR on the NAMMD timescale; the $^{\bullet}$S termini do not return into close enough proximity to attempt recoupling for the duration of the NAMMD simulation (Fig. 6).

For the remaining 43 systems, collision events can result in the compression of the nascent disulfide bond below the S_0 equilibrium bonded separation (Fig. 6). In this case, even if the system has already returned to the S_0 state, the $^{\bullet}$S termini are subject to an appreciable restoring force that can still spring the system back into the S_1/S_0 CR. The first collision event results in the compression of 19/43 systems by 0.32 ± 0.13 Å below the S_0 equilibrium bonded separation; although all 19 of these collisions occur on the S_0 surface, only three systems are able to balance the restoring force and remain in a ring-closed state; these systems do not re-enter the S_1/S_0 CR.

Furthermore, 2/50 systems are irreversibly damaged on photoexcitation; translocalisation of a radical site from one of the $^{\bullet}$S termini to a position on the carbon chain *via* atom abstraction prohibits further attempts at recoupling.

By 750 fs post-photoexcitation, the fraction of intact disulfides in the ensemble is consequently low. An appreciable (ps) lifetime ought to be expected for the ensemble. An approximate lifetime of 3.15 ± 0.22 ps (corresponding to depletion of the uncoupled diradical species down to 1/*e* of the initial population) is projected if the first collision event is assumed to be generally representative of all subsequent collision events and the rate at which the period of our motion lengthens is assumed to be constant. Stephansen *et al.*[15] report a lifetime of 2.75 ± 0.23 ps derived from one of the components of their ion current signal, in qualitative support of our projection and, by extension, our NAMMD result.

This is significantly slower than the timescale of internal conversion *via* photochemical funnelling in many natural systems, such as the DNA/RNA nucleobases,[28,29] and is likely also to be both slower and less efficient than the internal conversion processes protecting disulfides in proteins. For the latter systems, quite different behaviour to that revealed for 1,2-dithiane is anticipated, contrary to contemporary speculation.[9,15,16] It is conceivable that recoupling of the $^{\bullet}$S termini could theoretically take place on the ultrafast (fs) timescale if the peripheral parts of a protein limited the phase space that the $^{\bullet}$S termini could explore to the immediate area surrounding the equilibrium/Franck-Condon point. The internal conversion process would then be controlled by non-ergodic dynamics and limited only by how quickly the system could access the S_1/S_0 CR. In such a case, the S_1/S_0 MECI may also play a pivotal role in the internal conversion process, meriting further NAMMD studies on disulfides in rigid frameworks to address this question.

The photostability of 1,2-dithiane is a consequence of only loosely non-ergodic dynamics. The modest success of this approach hinges on the interplay between classical dynamics and quantum mechanics. Although advanced strategies are used industrially and in the natural world to engineer highly photostable structures, our NAMMD simulations highlight how small molecules continue to yield clever solutions.

Conclusions

A classically-intuitive reinterpretation of the internal conversion process in 1,2-dithiane has been revealed by our NAMMD simulations at the SA3-CASSCF(10,8) level and is communicated here ahead of our first ultrafast electron diffraction (UED) experiments[30,31] at the University of York. As ultrafast spectroscopic and spectrometric studies are only able to provide inferred information on the atomistic structures of systems under study, UED is the ideal approach to discriminate

between our interpretation of the internal conversion process and contemporary understanding since it allows for nuclear motion to be followed directly with sub-100 fs temporal and sub-Ångström spatial resolution.

The internal conversion process in 1,2-dithiane is assisted by a molecular "Newton's Cradle" with an average period of 349.6 fs. This motion is activated on disulfide bond fission, induced by absorption of light in the mid-UV, allowing the loosely non-ergodic exploration of phase space in an extensive S_1/S_0 coupling region associated with a high degree of multireference character and strong interstate coupling. The region can be entered as early as 65.0 ± 15.5 fs post-photoexcitation. Exploration of the region equilibrates the three lowest-energy singlet states and prepares an S_0-state ensemble in advance of periodic intramolecular collision events. These collision events can, under the right circumstances, restore the disulfide bond such that 1,2-dithiane appears photostable on the picosecond timescale.

Acknowledgments

We would like to thank the EPSRC (EP/I004122) for funding our research and both the EPSRC National Service for Computational Chemistry Software (NSCCS) and the staff at the York Advanced Research Computing Cluster (YARCC) for allowing us access to their computational resources. C.D.R. would like to thank Robin Virgo (University of York, Department of Chemistry) for many useful discussions.

Notes and References

All data created during this research are available by request from the University of York Data Catalogue; see DOI: 10.15124/6a57f11a-1056-456b-827f-9b7393c82c98

1 C. J. Reed, H. Lewis, E. Trejo, V. Winston and C. Evilia, *Archaea*, 2013, **2013**, 373275.
2 G. Cacciapuoti, F. Fuccio, L. Petraccone, P. Del Vecchio and M. Porcelli, *Biochim. Biophys. Acta,* 2012, **1824**, 1136-1143.
3 G. Cacciapuoti, M. Porcelli, C. Bertoldo, M. De Rosa and V. Zappia, *J. Biol. Chem.*, 1994, **269**, 24762-24769.
4 D. R. Boutz, D. Cascio, J. Whitelegge, L. J. Perry and T. O. Yeates, *J. Mol. Biol.*, 2007, **368**, 1332-1344.
5 C. Vieille and G. J. Zeikus, *Microbiol. Mol. Biol. Rev.*, 2001, **65**, 1–43.
6 T. R. Ioerger, C. G. Du and D. S. Linthicum, *Mol. Immunol.*, 1999, **36**, 373-386.
7 W. H. Qiu, L. J. Wang, W. Y. Lu, A. Boechler, D. A. R. Sanders and D. P. Zhong, *Proc. Natl. Acad. Sci.*, 2007, **104**, 5366-5371.
8 W. H. Qiu, T. P. Li, L. Y. Zhang, Y. Yang, Y. T. Kao, L. J. Wang and D. P. Zhong, *Chem. Phys.,* 2008, **350**, 154-164.
9 A. B. Stephansen, M. A. B. Larsen, L. B. Klein and T. I. Sølling, *Chem. Phys.*, 2014, **442**, 77-80.
10 P. M. Rao, J. A. Copeck and A. R. Knight, *Can. J. Chem.*, 1967, **45**, 1369-1374; K. Sayamol and A. R. Knight, *Can. J. Chem.*, 1968, **46**, 999–1003.
11 A. B. Callear and D. R. Dickson, *Trans. Faraday Soc.*, 1970, **66**, 1987-1995.
12 S. Nourbakhsh, C. L. Liao and C. Y. Ng, *J. Chem. Phys.*, 1990, **22**, 6587-6593.
13 C. W. Bookwalter, D. L. Zoller, P. L. Ross and M. V. Johnston, *J. Am. Soc. Mass Spectrom.*, 1995, **6**, 872-876.
14 C. Luo, W. N. Du, X. M. Duan, J. Y. Liu and Z. S. Li, *Chem. Phys. Lett.*, 2009, **469**, 242-246.
15 A. B. Stephansen, R. Y. Brogaard, T. S. Kuhlman, L. B. Klein, J. B. Christensen and T. I. Sølling, *J. Am. Chem. Soc.*, 2012, **134**, 20279-20281.
16 T. I. Sølling, T. S. Kuhlman, A. B. Stephansen, L. B. Klein and K. B. Møller, *ChemPhysChem*, 2014, **15**, 249-259.
17 J. C. Tully, *Faraday Discuss*., **1998**, 110, 407-419.
18 E. Tapavicza, G. D. Bellchambers, J. C. Vincent and F. Furche, *Phys. Chem. Chem. Phys.*, 2013, **15**, 18336-18348.
19 I. Taernelli, *Acc. Chem. Res.,* 2015, **48**, 792-800.
20 F. Weigend and R. Ahlrichs, *Phys. Chem. Chem. Phys.,* **2005***,* 7, 3297-3305.
21 M. Barbatti, G. Granucci, M. Ruckenbauer, F. Plasser, R. Crespo-Otero, J. Pittner, M. Persico, H. Lischka, NEWTON-X: A Package for Newtonian Dynamics Close to the Crossing Seam, Version 1.4, 2013, www.newtonx.org; M. Barbatti, G. Granucci, M. Persico, M. Ruckenbauer, M. Vazdar, M. Eckert-Maksić and H. Lischka, *J. Photochem. Photobio. A*, 2007, **190**, 228-240; M. Barbatti, M. Ruckenbauer, F. Plasser, J. Pittner, G. Granucci, M. Persico, and H. Lischka, *WIREs Comput. Mol. Sci.,* 2014, **4**, 26-33.
22 H. Lischka, R. Shepard, I. Shavitt, R. M. Pitzer, M. Dallos, T. Müller, P. G. Szalay, F. B. Brown, R. Ahlrichs, H. J. Böhm, A. Chang, D. C. Comeau, R. Gdanitz, H. Dachsel, C. Ehrhardt, M. Ernzerhof, P. Höchtl, S. Irle, G. Kedziora, T. Kovar, V. Parasuk, M. J. M. Pepper, P. Scharf, H. Schiffer, M. Schindler, M. Schüler, M. Seth, E. A. Stahlberg, J.-G. Zhao, S. Yabushita, Z. Zhang, M. Barbatti, S. Matsika, M. Schuurmann, D. R. Yarkony, S. R. Brozell, E. V. Beck, and J.-P. Blaudeau, M. Ruckenbauer, B. Sellner, F. Plasser, and J. J. Szymczak, COLUMBUS: An Ab Initio Electronic Structure Program, Release 7.0, 2015, www.univie.ac.at/columbus; H. Lischka, R. Shepard, R. M. Pitzer, I. Shavitt, M. Dallos, T. Müller, P. G. Szalay, M. Seth, G. S. Kedziora, S. Yabushita and Z. Zhang, *Phys. Chem. Chem. Phys.*, 2001, **3**, 664-673; H. Lischka, T. Müller, P. G. Szalay, I. Shavitt, R. M. Pitzer and R. Shepard, *WIREs Comput. Mol. Sci.,* 2011, **1**, 191-199.
23 R. Shepard, *Int. J. Quantum Chem.,* 1987, **31**, 33-44; R. Shepard, H. Lischka, P. G. Szalay, T. Kovar, M. Ernzerhof, *J. Chem. Phys.,* 1992, **96**, 2085-2098; H. Lischka, M. Dallos and R. Shepard, *Mol. Phys.,* 2002, **100**, 1647-1658.
24 H. Lischka, M. Dallos, P. G. Szalay, D. R. Yarkony and R. Shepard, *J. Chem. Phys.*, 2004, **120**, 7322-7329; M. Dallos, H. Lischka, R. Shepard, D. R. Yarkony and P. G. Szalay, *J. Chem. Phys.*, 2004, **120**, 7330-7339.
25 J. C. Tully, *J. Chem. Phys.,* 1990, **93**, 1061-1071; S. Hammes-Schiffer and J. C. Tully, *J. Chem. Phys.,* 1994, **101**, 4657-4667.
26 M. Barbatti, A. J. A. Aquino and H. Lischka, *Phys. Chem. Chem. Phys.,* 2010, **12**, 4959-4967.
27 W. C. Swope, H. C. Andersen, P. H. Berens and K. R. Wilson, *J. Chem. Phys.*, 1982, **76**, 637-649.
28 A. L. Sobolewski and W. Domcke, *Phys. Chem. Chem. Phys.,* 2004, **6**, 2763-2771.
29 C. E. Crespo-Hernandez, B. Cohen and B. Kohler, *Nature*, 2005, **436**, 1141-1144; C. E. Crespo-Hernandez, B. Cohen and B. Kohler, *Nature*, 2006, **441**, E8.

30 M. S. Robinson, P. D. Lane and D. A. Wann, *Rev. Sci. Instrum.*, 2015, **86**, 013109.
31 M. S. Robinson, P. D. Lane and D. A. Wann, *J. Phys. B: At. Mol. Opt. Phys.*, 2016, **49**, 034003.

